

A Monolithic Si Bolometer Array for the Caltech Submillimeter Observatory

Ning Wang, T. R. Hunter, D. J. Benford, E. Serabyn, T. G. Phillips
California Institute of Technology, M/S 320-47, Pasadena, CA 91125

S. H. Moseley

Laboratory for Extra Terrestrial Physics, Goddard Space Flight Center,
NASA, Code 690 Greenbelt, MD 20771

ABSTRACT

We are developing a submillimeter continuum camera for the Caltech Submillimeter Observatory (CSO) located on Mauna Kea. The camera will employ a monolithic Si bolometer array which was developed by Moseley *et al.* at the NASA Goddard Space Flight Center (GSFC). The camera will be cooled to a temperature of about 300 mK in a ^3He cryostat, and will operate primarily at wavelengths of 350 and 450 μm . We plan to use a bolometer array with 1×24 directly illuminated pixels, each pixel of dimension $1 \times 2 \text{ mm}^2$, which is about half of the F/4 beam size at these wavelengths. Each pixel is 10-12 μm thick and is supported only by four thin Si legs formed by wet chemical etch. The pixels are doped *n*-type by phosphorus implantation, compensated by boron implantation. Signals from the bolometer pixels are first amplified by cryogenically cooled FETs. The signals are further amplified by room-temperature amplifiers and then separately digitized by 16 bit A/D converters with differential inputs. The outputs of the A/D converters are fed into a digital signal processing board via fiber-optic cables. The electronics and data acquisition system were designed by the Goddard group. We will report the status of this effort.

1. INTRODUCTION

The measurement of radiation from interstellar dust is very important for the understanding of the physical and chemical processes in the interstellar medium. Currently continuum radiation from dust at millimeter and submillimeter wavelengths is measured using bolometers. In many astronomical studies, one needs to know the distribution of radiated flux from the interstellar dust. The Caltech Submillimeter Observatory (CSO) located on Mauna Kea presently uses a single pixel bolometer system. This system is equipped with optical filters for all atmospheric windows,

enabling one to measure dust continuum radiation from 1.3 mm to 350 μm . Large maps are often obtained using the "On The Fly" mapping routine.

We are developing a bolometer array system for the CSO. We plan to use a one dimensional monolithic Si bolometer array. The array will have 24 pixels, and will cover a field of view of 2 arcmin across the length of the array. In addition to the obvious improvement in mapping efficiency, the linear array may be used to develop better methods for elimination of potentially correlated low frequency fluctuations of the background atmospheric radiation.

Signals from the bolometers will be amplified using cryogenic FETs and room-temperature amplifiers. Data acquisition will be done using custom designed analog to digital converters (ADCs), and a digital signal processing (DSP) board inside a Macintosh computer.

In this paper, we will give a status report on the development of the array system. In section 2, we give a brief discussion of the Noise Equivalent Power (NEP) from the detector and from background fluctuations. In section 3, we describe the physical properties of the bolometer array. In section 4, we discuss the system's hardware, including electronics, data acquisition, and the optical system.

2. NOISE EQUIVALENT POWER

At the submillimeter wavelengths, the sensitivity of an ideal bolometric detector is limited by fluctuations in the background radiation. Assume that the telescope is pointed to a source which has a thermal emission temperature T_S , and that the source fills the diffraction beam. The signal to noise ratio of a bolometer at the telescope is given by ¹

$$S/N = \frac{2k_B T_S \Delta\nu \sqrt{\Delta t}}{NEP} \quad (1)$$

where $\Delta\nu$ is the bandwidth of the atmospheric window, Δt is the integration time, and NEP is the total noise equivalent power of the system. The NEP can be written as

$$NEP = \sqrt{NEP_{det}^2 + NEP_{bkgd}^2} \quad (2)$$

where NEP_{det} is the NEP of the entire detector system, including thermal fluctuations from the bolometer, noise from the amplifiers, and insufficient baffling of light leaks, and NEP_{bkgd} is the NEP from the fluctuations in the background radiation, which is given by

$$NEP_{bkgd} = \sqrt{\frac{4\epsilon h\nu k_B T_B \Delta\nu}{\eta} \left(1 + \epsilon\eta \frac{k_B T_B}{h\nu} \right)} \quad (3)$$

where ϵ is the sky's emissivity, ν is the radiation frequency, T_B is the temperature of the background radiation, and η is the quantum efficiency of the system, including imperfect passband transmission of the cryogenic filters, nonideal reflectance of the cryogenic mirrors, as well as the absorption efficiency of the bolometer. In Figure 1 we plot NEP_{bkgd} as a function of wavelength for three different quantum efficiencies, assuming $\epsilon = 0.5$, $T_B = 280$ K, and $\Delta\nu = 100$ GHz. We note that NEP_{bkgd} is greater than $2 \times 10^{-15} \text{ W}/\sqrt{\text{Hz}}$ from 200 to 800 μm .

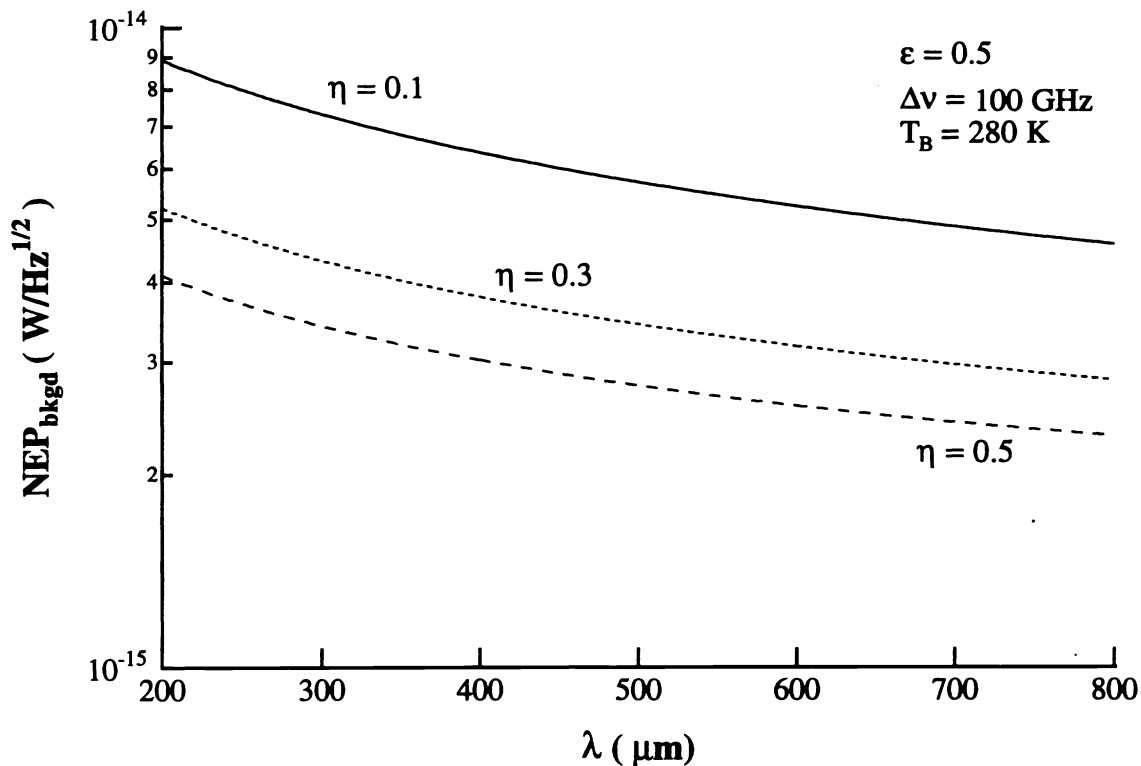


Figure 1. NEP_{bkgd} as a function of wavelength for three different quantum efficiencies. We have taken $\epsilon = 0.5$, $T_B = 280$ K, and $\Delta\nu = 100$ GHz. The NEP_{bkgd} given by this simple model is always above $10^{-15} \text{ W}/\sqrt{\text{Hz}}$.

It is important to point out that NEP_{det} is not independent of NEP_{bkgd} (see ref. 2). This can be understood as follows: the NEP_{det} varies inversely with the bolometer responsivity $\mathfrak{R} = \frac{T}{R} \frac{dR(T)}{dT}$, where R is the bolometer resistance and T is the bolometer temperature. The bolometer resistance typically depends on T through $R(T) = R_0 \exp(T_0/T)^\alpha$, where α is normally between 0.25 and 1, and R_0 and T_0 are constants. If the bolometer temperature is increased, the responsivity \mathfrak{R} will fall, increasing NEP_{det} . The dependence of NEP_{det} on NEP_{bkgd} comes about because increasing NEP_{bkgd} increases the incident radiation on the bolometer, which in turn increases the bolometer temperature; the NEP_{det} will then increase, following the above argument. Of course, Eq.3 is a very simple model. Nevertheless, Figure 1 gives us a good idea for the requirements on the detector NEP.

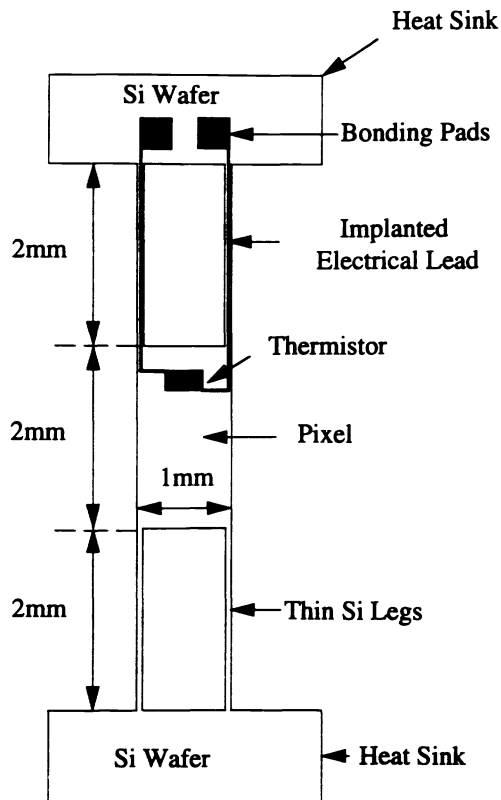
3. MONOLITHIC BOLOMETER ARRAY

The linear monolithic Si bolometer array that we plan to use was developed by Moseley *et al.*³ at the NASA Goddard Space Flight Center (GSFC). The bolometer pixels that make up the array are micromachined from Si wafers. Each pixel in the array is suspended by thin Si legs, which provide a weak thermal link from the bolometer to the thermal bath. A thermistor is formed by P implantation with B compensation, for each pixel.

In Figure 2 we show a schematic of a single bolometer pixel, where dimensions are 1mm \times 2mm \times 13 μm . There are four thin legs that support the pixel, with dimensions 12 μm \times 14 μm \times 2 mm. A thermistor is implanted in the pixel, and electrical contact is made by implanting P along two of the thin Si legs. Two metallic pads are deposited on the supporting frame of the Si wafer, and wires are ultrasonically bonded to these pads to connect the thermistor to the load resistor.

The 1 \times 24 array is shown in Figure 3, with a center to center spacing of just over 1 mm. Each bolometer pixel subtends 5 arcsec on the sky, which is half of the telescope beam size at 450 μm . We intend to operate this instrument primarily in the 350 μm and 450 μm atmospheric windows. This implies that along the long dimension of the array, we will achieve Nyquist sampling. The field of view along the array direction will thus be 2 arcmin.

The array has been installed in a single shot ^3He refrigerator which has a base temperature of about 320 mK. The zero bias resistance of the bolometer at base temperature was measured to be about $R_{\text{bolo}} = 3\text{--}4 \text{ M}\Omega$. A 30 $\text{M}\Omega$ load resistor, R_L , was used to bias each pixel. Connections from the load resistors and the array to the 4.2 K stage were made with 0.5 mil manganin wires to minimize thermal loads.



Note: The width of the thin Si legs have been exaggerated for the presentation.

Figure 2. A schematic drawing of a single bolometer pixel.

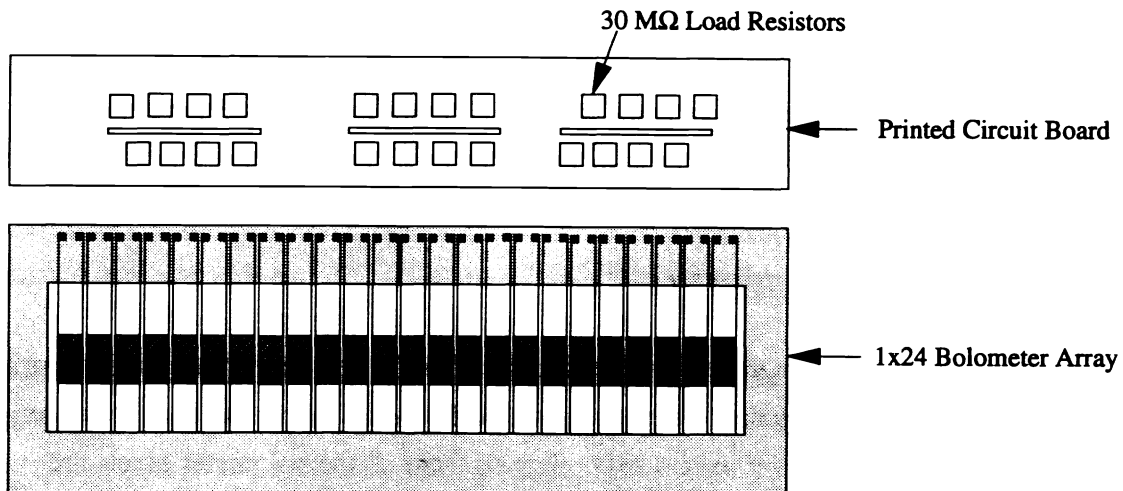


Figure 3. A schematic drawing of the 1x24 pixel array. For simplicity, wires are not shown in the drawing. Load resistors are grouped into three sets of eight resistors because eight channels share the same bias.

The load resistors reside on the same cold plate as the array, since $R_L \gg R_{\text{bolo}}$, the Johnson noise from these load resistors will be negligible. The NEP_{det} of the bolometer with no background radiation at the base temperature is expected to be around $2 \times 10^{-16} \text{ W}/\sqrt{\text{Hz}}$. For the wavelength range 350–450 μm and average viewing conditions on Mauna Kea, the instrument will be background limited, as demonstrated by Figure 1, as long as the bolometer is not heated significantly by the background radiation.

4. HARDWARE

4.1 ELECTRONICS

In order to minimize capacitive loading of the high impedance bolometers, we plan to use FETs as the first stage amplifiers. The FETs will be attached to the 4 K stage of the refrigerator. They will be suspended by Kevlar threads, so that self heating will maintain the FET temperature at about 120 K. This instrument will be used with a new chopping secondary mirror, where the chopping frequency will be about 3 Hz for a chop throw of 2 arcmin. Thus it is necessary to use FETs with low noise at 3 Hz. This will involve selecting FETs with a $1/f$ noise knee lower than 3 Hz.

Room temperature differential input amplifiers will be used to amplify the signal from the FETs before sending them to the ADCs. The amplifiers are based on a design by the GSFC group, with an AC gain of 500 and a DC gain of -0.5. The noise from these amplifiers is negligible compared to that from the cold FETs and the bolometers.

We are still in the process of selecting FETs with a $1/f$ knee lower than 3 Hz and a noise floor no higher than $15 \text{ nV}/\sqrt{\text{Hz}}$. We have built and tested a set of 24 room-temperature amplifiers for the 1×24 pixel array. We hope to test and assemble the FETs in the near future.

4.2 DATA ACQUISITION SYSTEM

The signals from the room temperature amplifiers will be digitized by ADCs, built from a design by the group at GSFC. They are 16 bit ADCs with differential inputs, with an input range of -3V to 3V. The sampling rate is set to be 1 kHz. Signals from all the bolometer pixels are digitized simultaneously, and then multiplexed before being sent to the DSP board.

In order to minimize the coupling of radio frequency (RF) noise into the bolometer system, we have installed RF filters on the cryostat; the insertion loss of these filters is 75 dB at 1 GHz.

Moreover, we are using fiber optic cables to carry the signal from the ADCs to the DSP to isolate the computer from the bolometer electronics.

The DSP board was built based on a design by A. Szymkowiak *et al.* ⁴, using a Texas Instruments TM320C50 DSP chip. It interfaces to a Macintosh, and resides in one of the expansion slots of a Macintosh IIvx. The primary function of the DSP board is to perform digital lock-in detection of the bolometer signal. A chop signal from the DSP board, which synchronizes with the ADC sampling clock, will be used to drive the chopping secondary mirror. The signal from the ADCs is demodulated according to a template function, returning in-phase and quadrature components, which are averaged over 8 chop cycles. Every bolometer pixel is allowed to have a different phase which the DSP takes into account when calculating the in-phase and quadrature components from each channel.

K. Boyce at GSFC has written a DSP driver, and software which interfaces the DSP board to the National Instrument's software development language Labview. All the data acquisition software is being written using Labview on the Macintosh. The Macintosh will serve the function of a backend computer; it will take data under the control of the VAX station 3100, the CSO's telescope control computer, using the TCP/IP protocol.

4.3. OPTICS

One of the unique features of this instrument is the lack of Winston cones. The light rays from the chopping secondary will be focused onto the bolometer pixels using off-axis mirrors placed inside the cryostat. The Cassegrain focus is reimaged by an off-axis elliptical mirror outside the dewar, placing an image of the primary on the low-pass filter at the dewar entrance. At the following focus inside the dewar, a slit at 4.2 K will be used as a cold baffle to stop the light leaks. The F/4 beam is then reimaged onto the array by off-axis mirrors inside the dewar. We have deposited a thin absorbing Bi film (about 1000 Å thick) on the back of each bolometer pixel. It has been demonstrated that for a given dielectric constant of the pixel material, with the proper resistance per square of the absorbing film, one can achieve frequency-independent absorption of up to 50% in the film ⁵. We are still in the design stage for the optical system. We hope to finalize the design in the near future.

5. CONCLUSION

In conclusion, we are developing a submillimeter linear bolometer array for continuum observations at 350 μm and 450 μm at the CSO. The array will be operated in a single shot ³He

refrigerator. We have started to measure the characteristics of the initial 1×24 pixel array, and have constructed and tested the data acquisition hardware, the ADCs and the DSP board, and the room-temperature amplifiers. The remaining tasks are to select, and to assemble the low temperature FETs, to fabricate the mirrors that will reside inside the refrigerator, and to write the data acquisition software.

6. ACKNOWLEDGEMENTS

We are very grateful to the group of people at GSFC, in particular to K. Boyce, and A. Szymkowiak. Without their help, this project would not have been possible. We also wish thank B. Mott and his staff in the microelectronics fabrication laboratory at GSFC, NASA, for fabricating the bolometer arrays and help us to bond the load resistors. This work is carried out under the NSF contract no: AST-9313929.

7. REFERENCES

1. T. G. Phillips, in *Millimeter and Submillimeter Astronomy*, p1-25, edited by R. D. Wolstencroft and W. B. Burton (Kluwer Academic Publishers, 1988).
2. J. C. Mather, *Applied Optics*, **23**(4), 584-588(1984).
3. S. H. Moseley, J.C. Mather, D. J. McCammon, *J. Appl. Phys.*, **56**(5) 1257-1262 (1984).
4. A. E. Szymkowiak, K. R. Boyce, R. G. Baker, S. H. Moseley, W. Folz, R. F. Loewenstein, *in preparation*.
5. J. Clarke, G. I. Hoffer, P.L. Richards, and N. -H. Yeh, *J. Appl. Phys.* **48**(12), 4865-4879(1978).